Prediction of Wear of Mill Lifters Using Discrete Element Method

Xiangjun Qiu, Alexander Potapov, Ming Song, Lawrence Nordell*
Conveyor Dynamics Inc.
*e-mail: qiu@conveyor-dynamics.com

September, 2001

ABSTRACT

3D-Discrete Element Method can be employed to simulate material wear inside of mining equipment. We introduce a new algorithm, which modifies existing DEM computer code to implement the well-known Archard's constitutive wear law. We show that the modified DEM program is able to predict wear behavior such as: wear shape, rate, and life. We further show that the DEM tool, with wear-prediction capability, can help to better design mining comminution components. The comparisons between measurements and predictions for the wear of mill lifters are presented in the paper.

INTRODUCTION

3D-Discrete Element Method (DEM) has been successfully employed in simulation of SAG, AG and ball mills to predict mill charge motion, power and energy spectra (Herbst and Nordell, 2001). In this paper, we try to explore a new application of 3D-DEM --- prediction of mill lifter and liner wear. For this purpose, we implement Archard's (1980) constitutive wear law in the DEM model. In the following sections, we will first discuss the theoretical background of implementing a DEM wear model. Then demonstrate the DEM capability of wear-prediction. We will show that the DEM with wear-simulation capability is able to predict worn lifter shape, wear rate and service life.

IMPLEMENTATION OF ARCHARD'S WEAR LAW

To date, numerous models for wear have been developed. In general, these models relate the volume loss of a material to load conditions on the surface of the material. Perhaps the most notable wear model is Archard's wear law. Archard's wear law takes the following mathematic form

$$V = K\ S\ P/H \qquad (1)$$

where V is the volume of material worn from the surface, S is the sliding distance, P is the shear force, H is the hardness of the material subjected to wear, and K is a constant. There are many other similar wear models developed. These models only try to express K as a function of specific surface conditions or load conditions. Rabinnowicz (1965) presented a model in which K of Eq.(1) is expressed in terms of the attack angle of abrasive particles. Zum Gahr (1988) developed a model, which takes into account material properties of work hardening, ductility and fracture toughness. Finnie (1972) proposed a special wear model, which addresses the erosion of a surface by a stream of solid particles. Although the original mathematic form of Finnie's model looks quite different from Eq.(1), it can be proven that Finnie's model reduces to Eq.(1) with K dependent on particle mass and moment of inertia. Due to its simplicity and generality, we only attempt to implement Archard's wear model in this paper. The validation of Archard's wear law in prediction of lifter wear will be further discussed in the following section. For implementation purpose, we rewrite Eq(1) in a form suitable for integration in a DEM model: i.e.

$$A\ dh = C\ dw \qquad (2)$$

where A is the surface area of a DEM element subjected to wear, and dh is the incremental loss of depth of the element, dw is the incremental shear work done on the surface area A, and C (equal to K/H) is defined as the wear rate. The implementation of Eq. (2) in a DEM program is simple and does not need further discussion. However, the selection of the wearing rate C is not straightforward and does need elaboration.

Since a typical SAG mill lifter can last for more than 10 months, it is not practical to try to simulate the actual period of wear life by using DEM. It is desirable that the DEM simulation time be shortened by several orders of magnitudes while the characteristics of the lifter wear are still captured by the model. For this purpose, we choose a wear rate in the simulation, denoted by C_{model}, which is several orders of magnitudes higher than the actual wear rate C of Eq.(2). Our experience shows that the suitable C_{model} must be determined by the following two rules:

1. C_{model} must satisfy the constraint of proportionality of Eq.(2). In other words, increasing the C_{model} by a factor of n and reducing the simulation time by the same factor must produce the same wear characteristics.
2. The entire simulation time must be sufficiently long that the statistical variance associated with discrete events is small in the DEM output data.

Both rule 1 and 2 are violated when a very large C_{model} is used in the simulation. Usually, a very large C_{model} will lead to a fast change of lifter geometry so that the mill charge motion will be strongly disturbed. The examples shown in the next section illustrates how to choose C_{model} for lifter wear. To distinguish it from the overall (macroscopic) lifter wear rate, we call C_{model} a microscopic wear rate.

VALIDATION OF WEAR MODEL

Once Archard's (microscopic) wear law is implemented in the DEM model, we can simulate the lifter wear in SAG, AG and ball mills. Our numerical results show that, in general, for most conventional types of lifers, the lifter cross-sectional area decreases almost linearly as mill running time increases (e.g. see Fig. 7). In other words, the macroscopic wear rate for a conventional type of lifter is constant in the simulation. We need to verify this by checking measured lifter wear data. In the measured data, any deviation from a constant lifter wear rate suggests that the Archard's wear law is invalid. Figure 1 shows a typical SAG mill with several lifter wear rates measurement corresponding to five different time periods. Obviously, the wear rates were not constant in these time periods. However, our further study shows that the ore hardness H_{ore} was not constant in the five periods (see Fig. 2). After introducing a correction factor, denoted by CT, for SAG operating time based on ore hardness, using an equation of the form $CT=a*H_{ore}^{b}$, the wear rates become surprisingly constant (see Fig. 3). This validates our adoption of Archard's model. It must be noted that the macroscopic wear rates for some non-conventional types of lifters (with novel geometry) may not be constant especially in their earlier stages of life.

Now let us explore what accuracy the DEM wear model can achieve. The example shown here is the simulation of a SAG mill lifter wear history. The results are shown in Fig. 4. The dashed lines represent the measured lifter profiles and the solid lines represent the DEM calculated profiles. In the simulation, the ratio of C_{model} /C is 1.7 $(10)^6$. The entire simulation period is less than 1.5 revolutions. The comparison between the simulations and measurements indicates that the DEM wear prediction is reasonably accurate.

The next example (shown in Fig. 5) demonstrates the effects of changing model wear rate C_{model} on simulation results. From Fig. 5, it is seen that when C_{model} /C is changed from 5 $(10)^5$ to 1 $(10)^6$ the simulated wear profiles coincide with each other very well. This means that rule 1 is obeyed. However, when C_{model} /C is increased to 1 $(10)^7$, the simulated wear profile significantly deviates from the profiles with C_{model} /C=5 $(10)^5$ and 1 $(10)^6$. and therefore rule 1 is violated.

EVALUATION OF LIFTER GEOMETRY

With the help of a DEM tool, which includes wear-prediction capability, we can evaluate different types of lifter geometries in terms of lifter life and mill comminution efficiency. In this paper, let us consider two types of lifters that are assumed to be installed in the SAG mills with the same operating conditions (e.g. mill diameter, number of lifters, mill speed, and holdup). One type of lifter is symmetrical with 30^O face angle ($2x30^O$) and runs in a bi-directional mode, and the other type is unsymmetrical with 30^O face angle ($1x30^O$) and runs in unidirectional mode. For the newly installed condition, both lifters have the same metal areas (mass) in their cross sections. We define a constant number of operating hours (say 750 hours) as one stage. After simulating four stages of wearing history, we demonstrate the results in Figs 6 to 10. Figure 6 shows the lifter profile evolution in the four stages. Figure 7 shows how the cross section area changes. We can see that the $1x30^O$ lifter wears faster than $2x30^O$ lifter. Figure 8 shows mill power draws corresponding to the two types of lifters. From this Figure, we see that the power draw corresponding to $1x30^O$ lifter type is larger, for most of its life cycle, than that corresponding to $2x30^O$ lifter type. Figure 9 illustrates the energy dissipated to particles in the mills with two different types of lifters. The SAG mill with $2x30^O$ lifter type has higher dissipated energy than the SAG mill with $1x30^O$. Figure 10 shows the energy utilization in SAG mills related with the two types of lifters, where the energy utilization is defined by the collisional energy divided by the power draw. From these results, we conclude that $2x30^O$ lifter type is better than $1x30^O$ lifter type.

This example demonstrates a specific condition. We do not suggest that proper design of a unidirectional mill cannot achieve, or exceed, the performance of a bi-directional mill. There are many important factors of lifter shape, comminution performance and wear life that are not addressed in this paper. Subtle modifications to the manufactured lifter shapes can produce significant improvements to life, power draw and comminution efficiency. Implementation of a DEM wear model validates comminution performance at a fraction of the cost, time, and risks spent on real mill modifications.

CONCLUSIONS

We demonstrate that DEM combined with Archard's wear law can be employed to simulate mill lifter wear. We find that the wear rate used in the DEM model can be several orders of magnitudes higher than the actual wear rate and the entire wearing process can be simulated within a few mill revolutions. Examples of lifter wear simulations show that such a modeling scheme still keeps a reasonable accuracy in comparison with measurements. We propose that DEM accurately replicates a mill's granular motions and forces by noted strong correlation between calculated and measured lifter wear morphology. We introduce two rules about the selection of model wear rate. Finally, we show that that the DEM tool with wear-prediction capability can help to better design mining comminution components.

References

1. Archard, J. F., 1980, "Wear Theory and Mechanisms", **Wear Control Handbook**, American Society of mechanical Engineers, New York,, pp. 35-80.
2. Finnie, I., 1972, "Some Observations on the Erosion of Ductile Metals", Wear, 19, pp81-90
3. Herbst, J. A. and Nordell, L., 2001, "Optimization of the Design of SAG Mill Internals Using High Fidelity Simulation", SAG 2001, Vancouver, B.C. October 2001
4. Rabinowicz, E., 1965, **Friction and Wear of Materials**, Wiley, New York.
5. Zum Gahr, K. H., 1988, "Modeling of Two-Body Abrasive Wear", Wear, 124, pp. 87-103

Acknowledgements

The authors gratefully acknowledge the assistance of J.A. Herbst in the preparation of this manuscript. A portion of the work performed here was done under the sponsorship of Svedala Optimization Services.

Figures

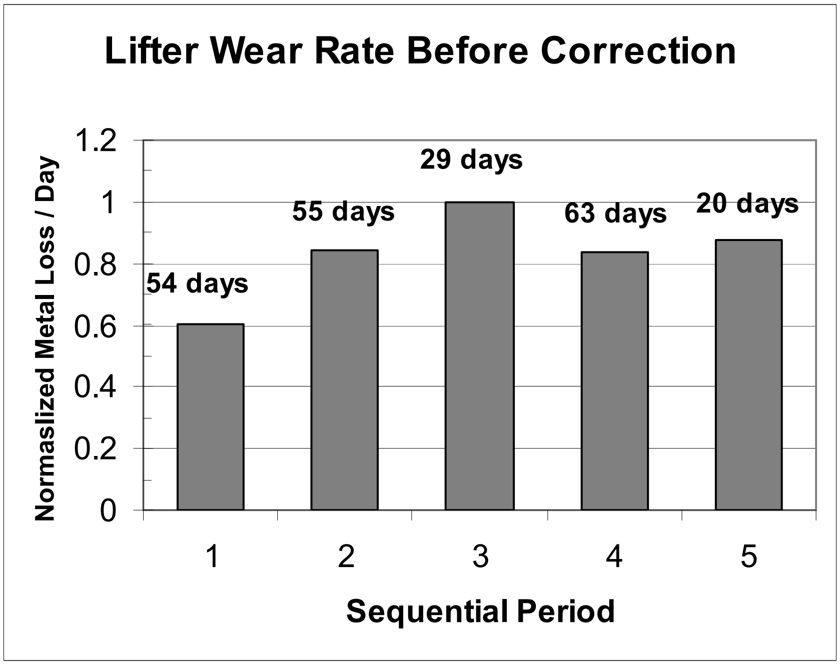

Fig. 1 Measured SAG Mill Lifter Wear Rate Before Correction
Period 1: 0-54days; Period 2: 55-109 days; Period 3: 110-138 days; Period 4: 139-201 days; and Period 5: 202-221 days.

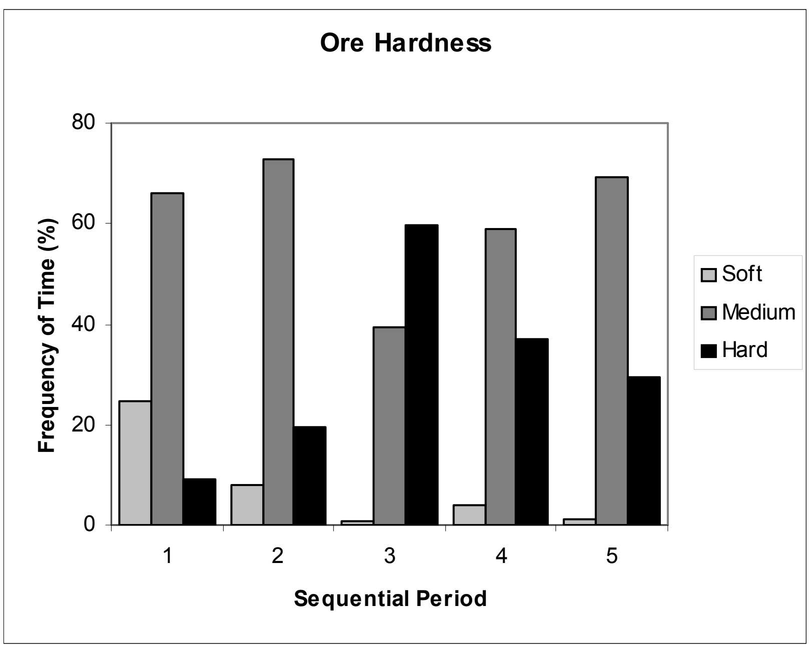

Fig. 2 Ore Hardness

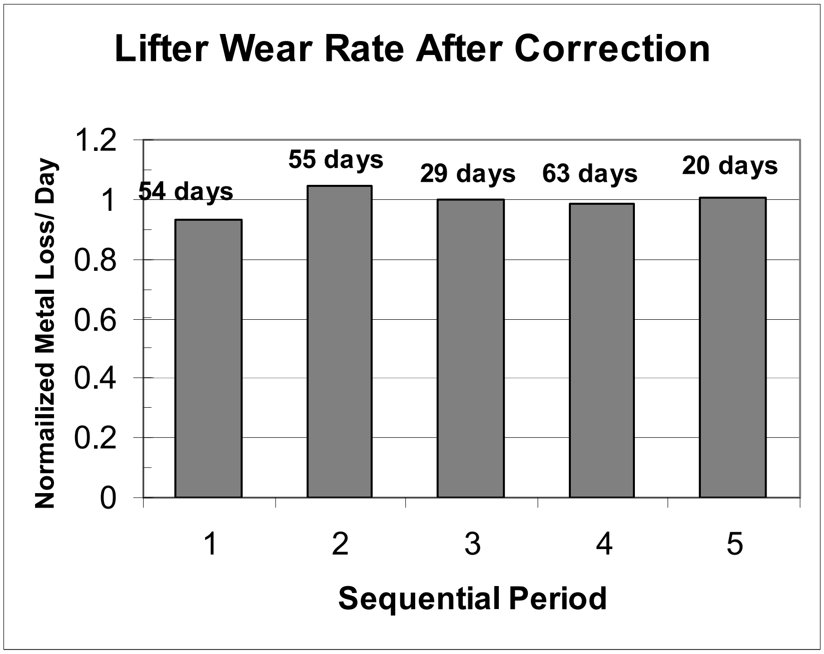

Fig. 3 Measured SAG Mill Lifter Wear Rate After Correction

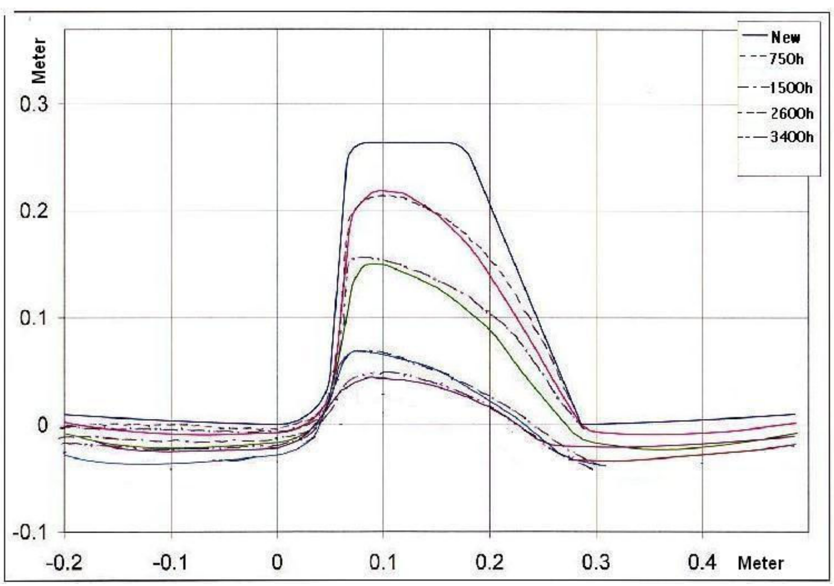

Fig.4 Simulation and Measurement of SAG Mill Lifter Wear History

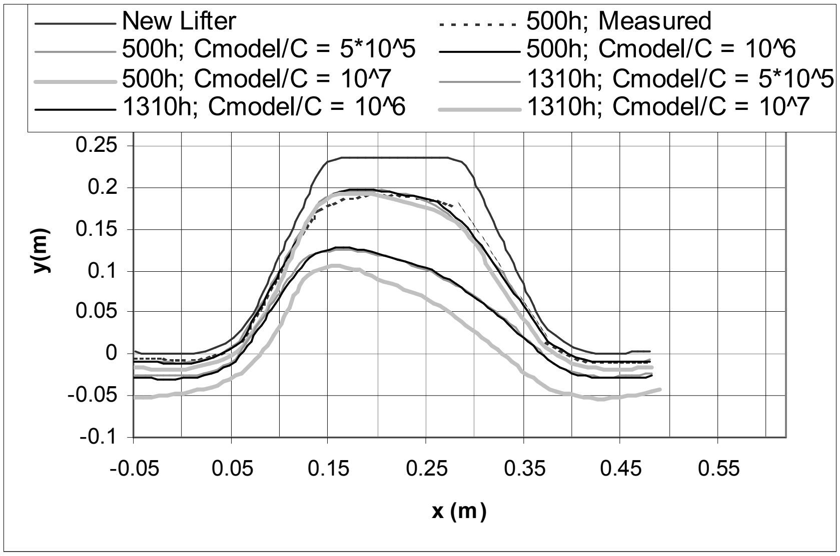

Fig.5 Effect of Selection of C_{model} on Simulation Accuracy

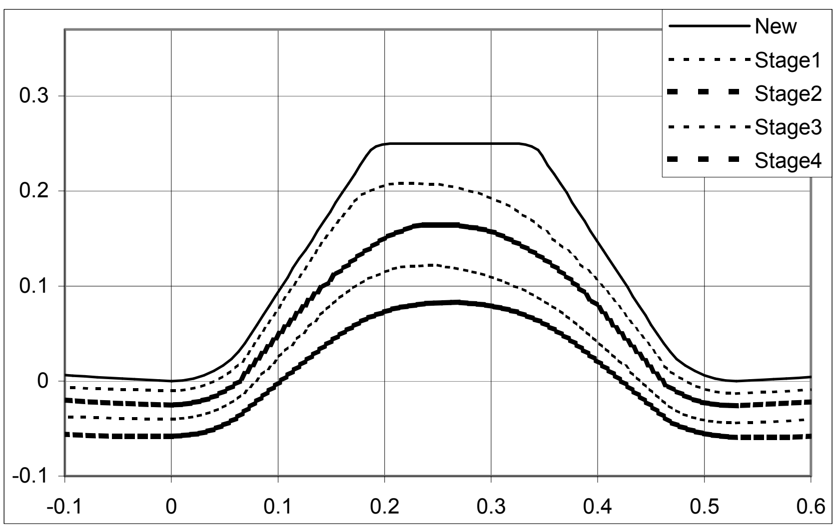

Fig.6a SAG Mill 2x30^{O} Lifter Wear History, (Unit of coordinates: Meter)

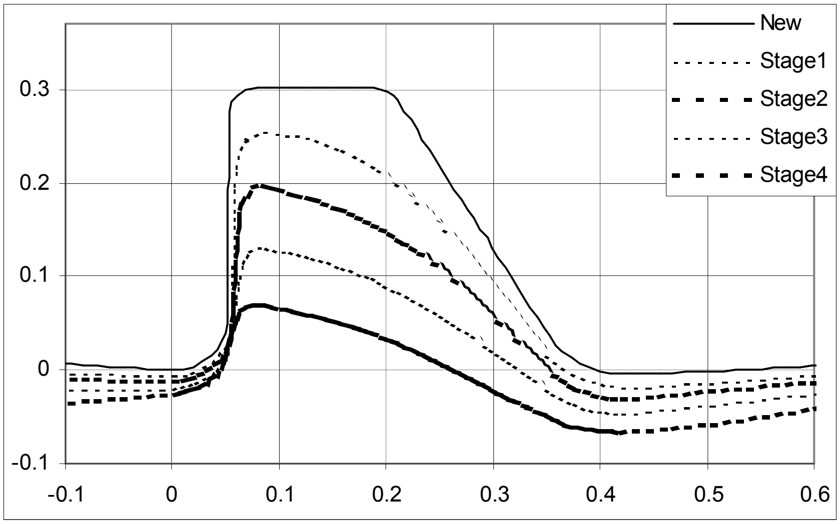

Fig.6b SAG Mill 1x30^O Lifter Wear History, (Unit of coordinates: Meter)

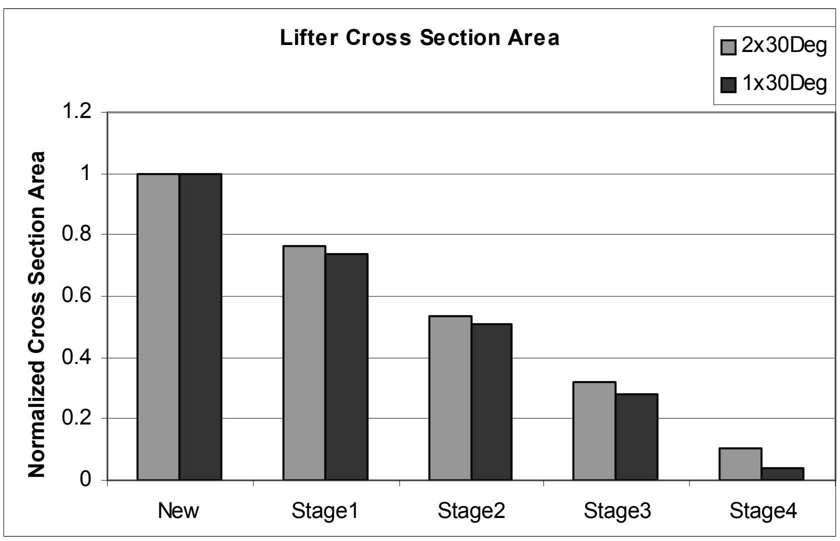

Fig. 7a Lifter Cross-Section Areas Normalized with respect to the Cross-Section Area of New Stage

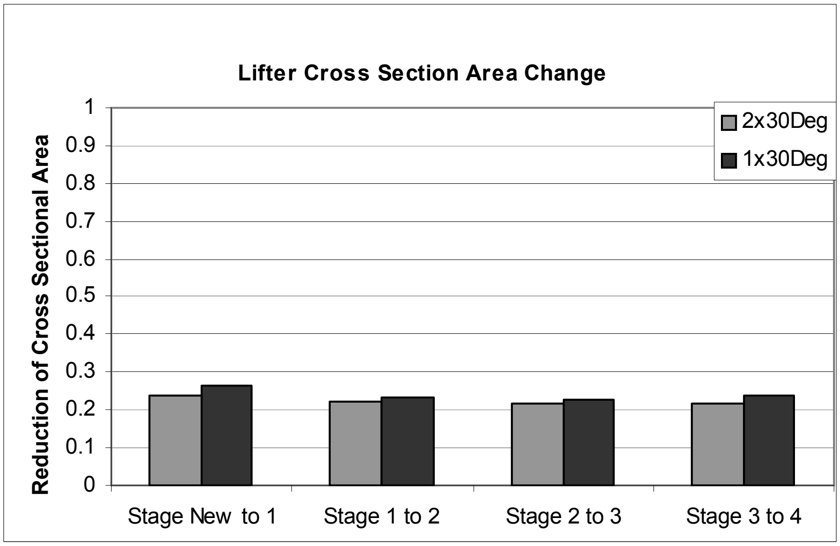

Fig. 7b Lifter Cross-Sectional Area Reduction with respect to the Cross-Section Area of New Stage

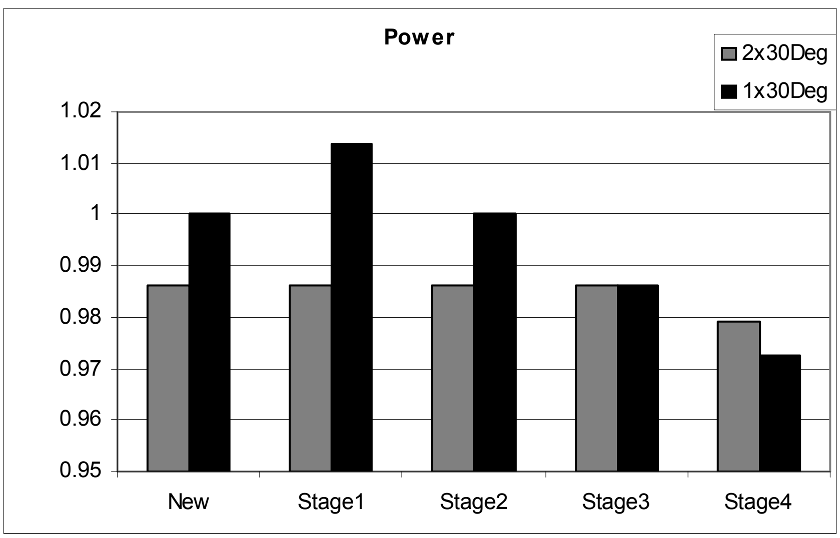

Fig.8 SAG Mill Power Draw Normalized with respect to that of $1x30^{O}$ New Stage

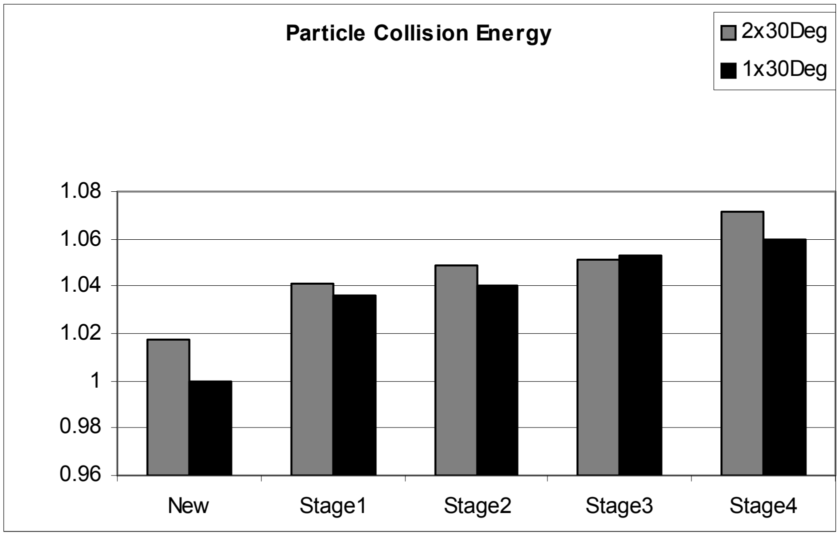

Fig.9 Particle Collision Energy in SAG Mill Normalized with respect to that of $1x30^{O}$ New Stage

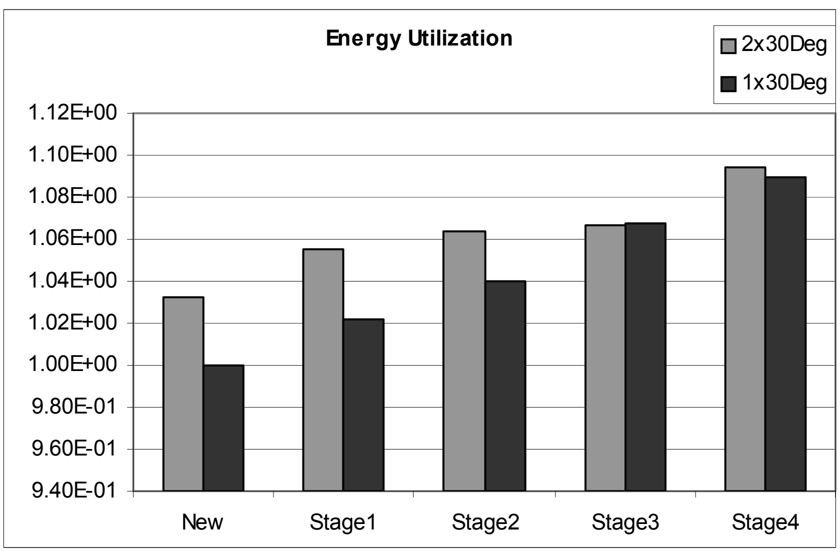

Fig.10 SAG Mill Energy Utilization Normalized with respect to that of $1x30^{O}$ New Stage